Structural Characteristics of the Tubular Conical-Helix of Graphitic Boron Nitride

F. F. Xu*,†,‡ and Y. Bando‡

Shanghai Institute of Ceramics, 1295 Dingxi Road, Shanghai 200050, China and National Institute for Materials Science (NIMS), 1-1 Namiki, Tsukuba, Ibaraki 305-0044, Japan

Received: July 6, 2004; In Final Form: September 21, 2004

Electron diffraction and high-resolution electron microscopy have been used to investigate the structures of the tubular conical−helix of graphitic boron nitride. An ordered interlayer structure showing a certain coincidence site lattice has been documented by electron diffraction. Meanwhile, the graphite-type *ABAB* packing was observed in this BN nanostructure, indicative of an actual wrapping performance around a 120° symmetry position and the dominant role of the density rather than the type of interlayer interaction in the interlayer configuration. Finally, structural elements defining the complete structure of a conical−helix have been summarized and discussed.

Introduction

Recently, we reported a novel nanotubular form of graphitic boron nitride (BN), which shows the geometry of an Archimedes spiral or a conical−helix (see Figure 1).[1−4] Unlike the solid BN or C graphitic cones which were considered to form following the creation of a topological defect at the conical apex,[5−11] the as-obtained helical−conical nanotubes (HCNT) were generated via wrapping a single beltlike BN filament onto the curved surface of a preformed BN microstructure, namely, microworm.[1] The absence of the apical regions in successive helical-packed monolayer cones eventually leads to a hollow channel at the center of the one-dimensional nanofiber and hence the occurrence of an additional form of filamentary nanotubes.

The graphitic HCNT resembles a molecular spring composed of a single filamentary screw with an atomic ranged screw-pitch equaling $d_{002}/\sin(\theta_{apex}/2)$, where d_{002} is the interspace of stacking filaments, i.e., 0.334 nm for graphitic BN, and θ_{apex} is the apex angle of the cone. Thus, HCNTs have a spring-like structure and actually behave like a spring,[2] which exhibited striking flexibility and elasticity. In-situ transmission electron microscopy showed that the nanotubes could bear extremely high strain at room temperature,[2] which, to date, has only been observed in metals or plastics. Moreover, the deformed nanotubes retrieved starting morphology without any structural defects produced as soon as the exterior stress was released. The outstanding structural property is attributed to both the high stiffness of BN filaments and the enhanced interlayer slide in helical cones. The high curvature in HCNT is considered to be stabilized by the interlayer bonding determined by the density of coincidence lattice sites (CLS) or the size of coincidence site lattices (CSL).[3,6,7] The further weakened interlayer interaction for a CSL which is usually several times larger than the graphitic unit cell allows an easier interlayer sliding upon exterior stress. Moreover, it has been found that thermal treatment also provides the driving force for the interlayer slide, through which structural reconstruction is performed, giving a well-defined structural configuration, e.g., cone apex angle (θ_{apex}) and overall bending curvature, determined by the temperature.[1] Therefore, material design and the possible control of properties appear practicable for this filamentary nanotube. These unique structural properties highlight its application potentials in, for example, field emission and high-performance structural materials.

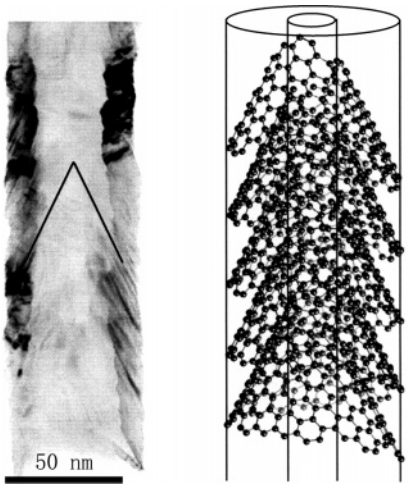

Figure 1. Electron micrograph of a BN HCNT and its structural model.

Before attempting to determine the effects of structural elements, e.g., cone apex angle and CSL, on the physicochemical properties of BN HCNTs, a good understanding of their structures is required. Theoretically, HCNT broadens the structural configurations of conical−helix via introduction of disclination operations around a 3-fold symmetry position, i.e., an individual atom in addition to the 6-fold symmetry site, i.e., the center of an individual atomic hexagon.[3] Through these additional disclination operations some new packing structures occur. For example, a graphite-type *ABAB* packing appears in a 180° disclinated BN cone if wrapping performance is undertaken around a 3-fold axis. In this paper, transmission electron microscopy is applied to the investigation of the structures of BN HCNTs, including their electron diffraction patterns and high-resolution electron microscopy (HREM) images. The actual formation of CSLs is evidenced by electron diffraction. A disclination performance around a 3-fold axis is

* To whom correspondence should be addressed. Phone: +86-21-52413104. Fax: +86-21-52412574. E-mail: ffxu@mail.sic.ac.cn.
† Shanghai Institute of Ceramics.
‡ National Institute for Materials Science (NIMS).

10.1021/jp047011p CCC: $27.50
Published on Web 11/13/2004

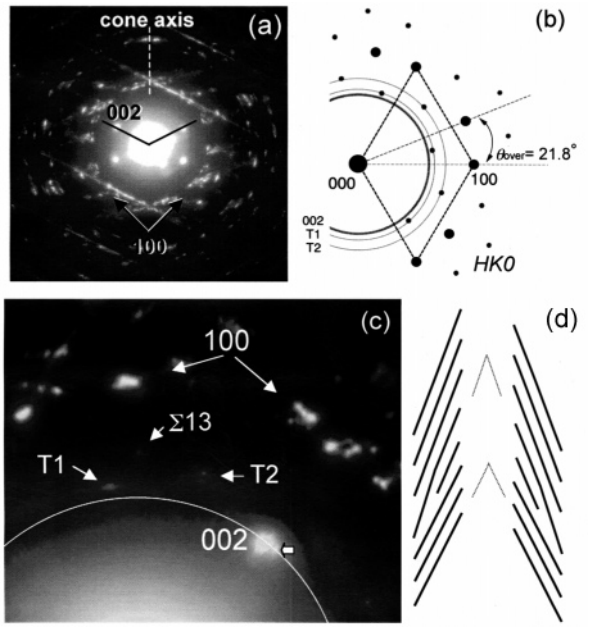

Figure 2. (a) Electron diffraction pattern of an individual HCNT. (b) Schematic drawing of the reciprocal space for a Σ7-CSL ordered packing structure. The curves indicate the positions of the corresponding main reflections, i.e., (002) and *HK0* satellites, would appear. (c) The observed electron diffraction pattern where weak satellites belonging to Σ7 (T1 and T2) and Σ13 are discernible. The fragment of a drawing circle refers to the positions that a reciprocal vector (002) may appear. (d) Shortening of the local belt width leads to a change in the apex angle and hence the coexistence of different ordered packing structures.

also observed. It will be seen that HCNT should be regarded more as a molecule than as a crystal. Moreover, small fluctuation prevails in the observed HCNT structure, which results in local modification of packing pattern and CSLs, and a small change in regional apex angle, hence a lower grade of structural rigidity and periodicity. Finally, structural elements defining the HCNT structure are summarized and discussed.

Experimental Section

The synthesis of BN HCNTs involves two heating stages with starting materials B_2O_3 and carbon nanotubes (CNT) in a N_2 atmosphere. A preheating process at 1700 °C generated an intermediate microproduct, namely, microworm. BN HCNTs then grew onto the curved surfaces of microworms at an elevated temperature (1800 °C). Details of the synthesis have been described in our recent work.[1] Structural analyses including electron diffraction and high-resolution electron microscopy were performed on a JEOL3000F field-emission transmission electron microscope operated at 300 kV. Image simulation was done on a MacTempas platform.

Results and Discussion

The typical diffraction pattern of a helical cone consists of two rows of 00*l* reflections meeting at an angle equal to 180° − θ_{apex} and *hk*0 arcs along the direction perpendicular to the cone axis.[9] Figure 2a shows the electron diffraction pattern of an individual BN HCNT when the cone axis is, to the extreme extent, perpendicular to the incident beam. This could be easily and quickly achieved according to the method developed by L. Bourgeois.[9] The real apex angle meets the minimum observed angle through tilting the nanotube around the normal of the tube axis. The as-obtained diffraction pattern displays sharp intersection of *hk*0 arcs on the pathway of the cone axis, while a pair of hyperbola-like curves otherwise appear at the intersection if the cone axis is not critically perpendicular to the incident beam. The measured apex angle in Figure 2a is 52°, which corresponds to a disclination angle of 180° + 21.8°.[3,5−7] Since an overlap angle (θ_{over} = 21.8°) is involved in the disclination operation, the observed tubular cone shows a helical nature[3,5−7] as modeled in Figure 1b. Theoretically, this overlap angle refers to a Σ7 CSL interlayer structure.[3] However, it is generally very difficult to obtain direct evidence of whether the ordered overlap configuration really applies. The CSLs in a helical cone can hardly be observed by, for example, HREM because they also rotate upon wrapping of the filament. The CSLs obtained between the second and the third overlapping layers involve an additional rotation of θ_{over} with respect to those for the first two overlapping sheets (Figure 3). If taking into account all three overlapping layers, we observe an enlarged second-order CSL (marked by asterisks in Figure 3) which can be described as $\Sigma\sigma^{n-1}$ CSL. Here, $\Sigma\sigma$ denotes the initial CSL for a certain θ_{over}, e.g., Σ7 or Σ13, etc., and *n* refers to the number of overlapping layers. The overlapping structures tend to be more complicated and the size of overall CSL (*n* − 1 powers of the size of initial CSL) becomes fairly large with an increase in the number of packing layers, hence the poor crystallinity inherent in HCNT. Therefore, neither graphitic nor CSL structure is discernible in an HREM observation. However, our present study finds that CSL configuration can be detected by electron diffraction.

For a perfect ordered packing structure, i.e., a CSL, in a conical−helix, an additional CSL (*HK*0 satellites in Figure 2b) locus superimposes onto each *hk*0 locus in reciprocal space. As a result, fringe-like *HK*0 arcs appear, extending parallel to the *hk*0 arcs on the diffraction pattern. The interspaces between *HK*0 and *hk*0 arcs refer to the size of CSL. In the TEM observation we could not observe *HK*0 arcs but weak reflection

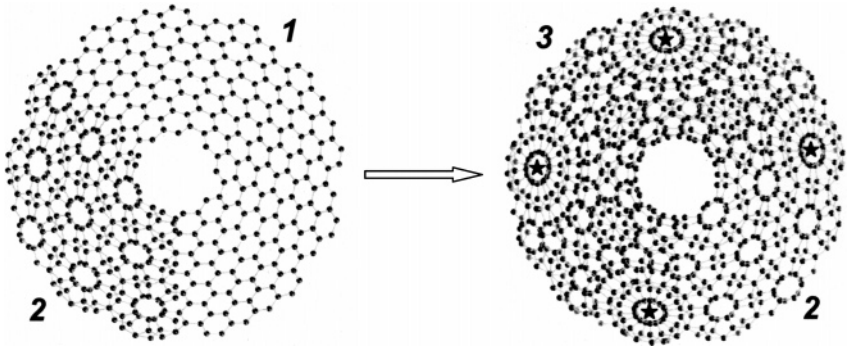

Figure 3. Wrapping of filament brings about a simultaneous change in CSL patterns, indicating a molecular rather than a crystalline nature of HCNT. The digits refer to the number of overlapping layers.

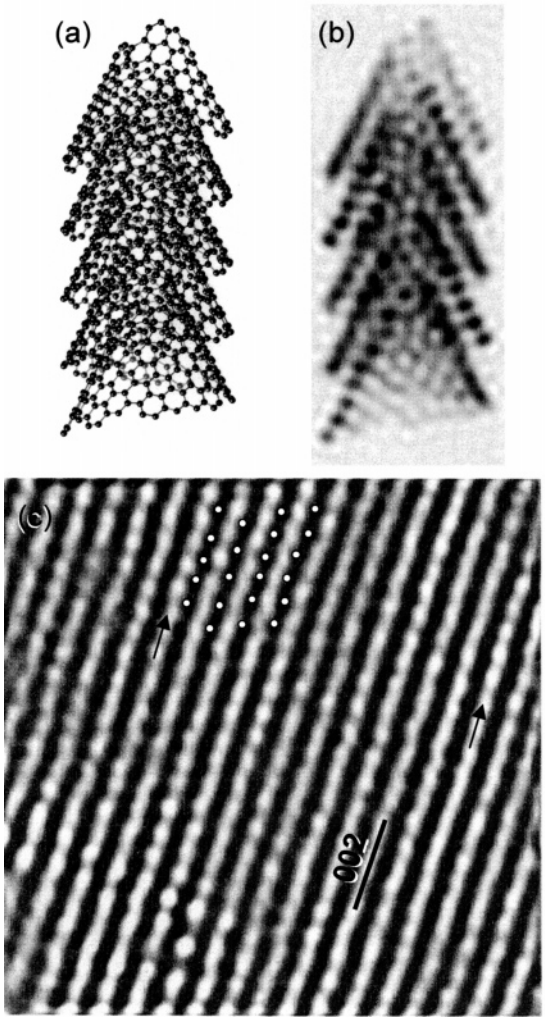

Figure 4. Structural model (a) and its calculated structural image (b) of a $\theta_D = 180 + 21.8°$ HCNT. (c) The observed HREM image of a BN HCNT, which shows an irregular dot−bar pattern and a plausible superperiodic structure.

spots or stripes in the vicinity of the *hk*0 arcs as seen in Figure 2c. It is noted that the Σ7 CSL has an area seven times the basic BN unit cell. In the direction of an incident beam, Σ7 CSL displays a smaller possibility for certain *HK*0 lattice vectors to favor the Bragg conditions. For a thin-walled nanotube, the selection rule further restricts the number of *HK*0 reflections and hence the discreteness of *HK*0 reflections on the diffraction pattern. By superimposing predicted positions (Figure 2b) for a Σ7 CSL on the diffraction pattern (Figure 2c), good agreement is obtained associated with the reflection positions (referring to the size of CSL) and the distribution of these *HK*0 satellites (T1 and T2). A critical correlation between the observed apex angle and the predicted CSL is evidenced. Therefore, helical cones actually employ ordered interlayer packing, which is ascribed to the high density of coincidence lattice sites. CLSs provide a sole 'strong' interlayer interaction that guarantees the stabilization of such a highly curved filamentary structure. The faint reflection in Figure 2c may indicate the local existence of a larger Σ13 CSL in an otherwise perfect Σ7 CSL-stabilized HCNT. Σ13 CSL is formed via an overlap angle of 27.8°.[3] In this case, the 6° discrepancy in the disclination angle results in a difference of the apex angle of 2°. A less strong reflection spot (marked by an arrow in Figure 2c) appears in close vicinity of the main (002) reflection, which shows a ∼2° discrepancy in apex angle. Two possible reasons may interpret the coexistence of different apex angles within an individual nanotube. A structural defect (Figure 2d) similar to the edge dislocation brings on the change of the apex angle. At any rate, the wrapping filamentary belt does not break but remains continuous through the defect, which was created simply due to a shortening of belt width. The other factor that may change the apex angle relies on slight bending of the nanotube. Local structural collapse or cleavage, which can also modify the apex angle, has not been observed.

Unlike the cylindrical BN nanotubes, an HCNT displays the HREM image showing dot patterns characteristic of neither hexagonal nor rhombohedral symmetry. Figure 4a and b illustrates the structural model of a $\theta_D = 180° + 21.8°$ HCNT and its calculated HREM image. The distribution of atomic potentials projecting along the normal of the nanotube axis is of poor regularity. The dark dots represent the sum of the contributions from all atoms within the point-resolution (for TEM) range (typically less than 0.2 nm) along the view direction rather than an atomic column as in cylindrical nanotubes. Therefore, the distribution and shape of dark dots are usually irregular. They either displace along the sheet normal, displaying a wavy fringe lattice, or coalesce to form bars on a sheet plane. The observed image (Figure 4c) shows a similar irregular dot pattern. It has been cited that a well-ordered overlapping structure determined by a certain θ_{over} or CSL should display a corresponding long periodicity (p) normal to the sheet, which is obtained by $p\theta_{over}/q = k60°$.[11] For $\theta_{over} = 21.8°$, every 11 layers ($p = 11$, $q = 1$, and $k = 4$) will cause reappearance of a certain edge-on *hk*0 lattice image. Our HREM observation reveals a plausible match with the expected periodicity (marked by arrows in Figure 4c). In any case, different bending curvature along the sheet normal inhibits occurrence of a perfect long periodicity. HCNT should be regarded more as a molecule than as a crystal.

The structure of a tubular conical−helix is fully determined by four elements: the disclination angle; the wrapping mode, i.e., the symmetry position around which wrapping is performed;[3] the tubular radius and wall thickness; and finally, the handedness of rotation. The first two elements dominate the apex angle and the packing pattern or CSL of the helical cone. Our recent work summarized conical−helix structures by taking into account these two structural elements.[3] It has been found that a wrapping performance around a 120° symmetry position, i.e., an individual atom, will display a graphite-type *ABAB* packing pattern if the disclination angle equals $(2k + 1)60°$. Such graphite-type packing structure in a BN system has been observed in the present study. Figure 5 shows the electron diffraction pattern and the HREM image of an HCNT with a disclination angle of 180° or an apex angle of 60°. The lattice image (Figure 5b) displays a typical *ABAB* packing pattern. It has been noted that the disclination angle of multiples of 60° may refer to either nonhelical or helical conical configuration.[3] Nevertheless, no *ABAB* but only favorable *AA′AA′* (Hex) or *ABCABC* (Rhomb) is observed in nonhelical BN cones, where the packing pattern is fixed at the nucleation stage and will not change during and after growth. Even if a fault, e.g., *ABAB* packing, occurs, this faulted pattern may involve a very small volume because it is energetically unfavorable in the BN structure. Each monolayer cone packs independently over one another in a stacked cone and can easily avoid further packing of this unfavorable configuration. However, in helical cones, overlapping layers are interconnected via introduction of a screw dislocation. The structure consists of a single continuous filament with a narrow belt-like morphology. Therefore, a small

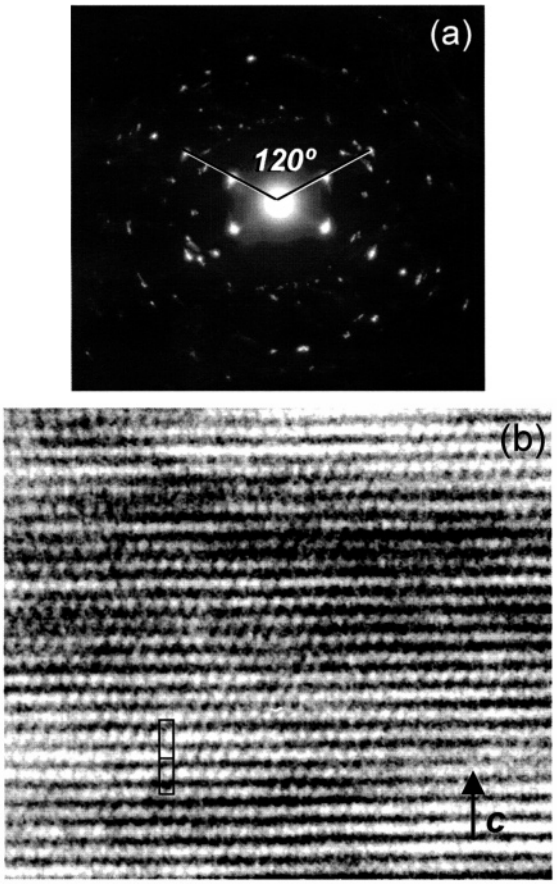

Figure 5. (a) Electron diffraction of a 180°-disclinated ($\theta_{apex} = 60°$) HCNT. The HREM image (b) shows a graphite-type *ABAB* packing, indicating an actual wrapping performance around a 3-fold axis.

lattice displacement, for example, 1/3⟨210⟩, will lead to a change in the whole overlapping structure, giving rise to modification of stacking from *AA′AA′* to *ABAB* in the continuously packed filaments until an additional lattice displacement is introduced. Thus, we believe that we observed a wrapping performance about a 3-fold axis, which is one of the rare cases (i.e., only for $(2k + 1)60°$ disclination) that could be clarified. For disclination operation involving an additional θ_{over}, currently no available techniques can identify the symmetry position for wrapping. It should be noted that the observed *ABAB* packing could be a defective region (formed by a 1/3⟨210⟩ displacement from the *AA′AA′* stacking mode), though it involves a large section along the nanotube. Albeit less favorable than *AA′AA′* stacking in energetic consideration, *ABAB* packing still provides a higher density of coincidence lattice sites than CSLs in a conical−helix. This is additional evidence to our recent consideration[3] that the density rather than the type of interlayer interaction dominates the packing structure in helical cones. Thus, for a conical−helix with a disclination angle of $n60° \pm \theta_{over}$, the integer *n* that largely defines the overall bending curvature is determined by the temperature[1] while θ_{over} that dominates the interlayer packing structure is chosen according to the criteria that it can provide the density of coincidence lattice sites in order to compete with the curvature strain.

Among the four structural elements, the handedness of rotation is possibly the most important one for a conical−helix. Wrapping of filament can be performed in either a right-handed or left-handed fashion, which are related by a mirror reflection as seen in Figure 6. In organic chemistry, ring-shaped carbohydrates may show completely different properties by an inverse in handedness of rotation. This effect could be enhanced if doping or adsorption is involved in this low-symmetrical structure. Presently, finding a way to identify the handedness of rotation in an individual conical−helix is highly desired. Further theoretical and experimental work is required to investigate whether and how these structural elements influence the properties of HCNTs.

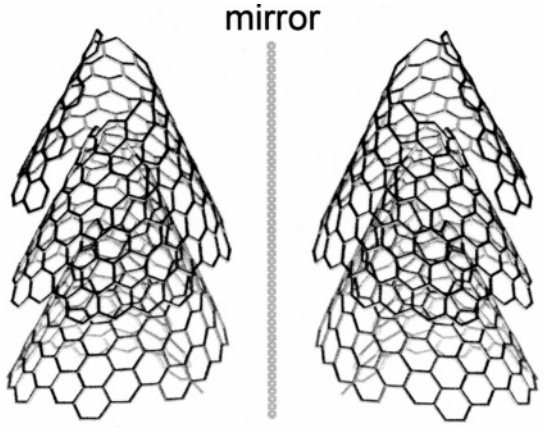

Figure 6. Mirror-reflected handedness of rotation: right-handed (left) and left-handed (right).

Conclusions

The structures of a tubular conical−helix of graphitic boron nitride have been examined by transmission electron microscopy. Actual ordered interlayer packing, i.e., CSL, has been evidenced by electron diffraction. High-resolution electron microscopy observed a graphite-type *ABAB* packing in an otherwise unfavorable BN system. Thus, for a conical−helix with a disclination angle of $n60° \pm \theta_{over}$, the temperature determines the integer *n* that largely defines the overall bending curvature, while θ_{over}, which dominates the interlayer packing structure, is chosen according to the criteria that it can provide the density of coincidence lattice sites irrespective of the packing type in order to compete with the curvature strain.

Acknowledgment. We thank Drs. D. Golberg, R. Z. Ma, Y. B. Li, C. C. Tang, and M. Mitome in NIMS for assistance in the experimental work.

References and Notes

(1) Xu, F. F.; Bando, Y.; Ma, R.; Golberg, D.; Li, Y.; Mitome, M. *J. Am. Chem. Soc.* **2003**, *125*, 8032.
(2) Xu, F. F.; Bando, Y.; Golberg, D.; Ma, R.; Li, Y.; Tang, C. C. *J. Chem. Phys.* **2003**, *119*, 3436.
(3) Xu, F. F.; Bando, Y. *Acta Crystallogr., Sect. A* **2003**, *59*, 168.
(4) Xu, F. F.; Bando, Y.; Golberg, D. *New J. Phys.* **2003**, *5*, 118.
(5) Double, D. D.; Hellawell, A. *Acta Metall.* **1974**, *22*, 481.
(6) Amelinckx, S.; Luyten, W.; Krekels, T.; Van Tendeloo, G.; Van Landuyt, J. *J. Cryst. Growth* **1992**, *121*, 543.
(7) Amelinckx, S.; Devouard, B.; Baronnet, A. *Acta Crystallogr., Sect. A* **1996**, *52*, 850.
(8) Krishnan, A.; Dujardin, E.; Treacy, M. M. J.; Hugdahl, J.; Lynum, S.; Ebbesen, T. W. *Nature* **1997**, *388*, 451.
(9) Bourgeois, L.; Bando, Y.; Shinozaki, S.; Kurashima, K.; Sato, T. *Acta Crystallogr., Sect. A* **1999**, *55*, 168.
(10) Bourgeois, L.; Bando, Y.; Han, W. Q.; Sato, T. *Phys. Rev. B* **2000**, *61*, 7686.
(11) Bourgeois, L.; Bando, Y.; Kurashima, K.; Sato, T. *Philos. Mag. A* **2000**, *80*, 129.